

Synchronization Phenomena in Coupled van der Pol Oscillators Containing Three Oscillators with Star Structure Connected to Another Oscillator

Vu Minh Hien, Yoko Uwate and Yoshifumi Nishio

†Dept. of Electrical and Electronic Engineering, Tokushima University,
2-1 Minamijosanjima, Tokushima, 770-8506 Japan
Email: {hien, minhhai, uwate, nishio}@ee.tokushima-u.ac.jp

Abstract

In this study, synchronization phenomena in coupled oscillators containing star structure connected to another oscillator is investigated. We focus on the phase difference between two oscillators when coupling strength is changed. By using computer simulations, we observe synchronization phenomena of the system and use theoretical analysis and circuit experiment to confirm computer simulation results.

1. Introduction

We are living in the world where there are so many example of synchronization: firefly luminescence, cry of birds and frogs, human applause, etc. Synchronization phenomena have a long history of researches and they have been reported in many researches of engineering fields [1] - [2]. Furthermore, the applications of synchronization phenomena have been also found in chemical, physical and biological fields [3] - [4]. Synchronization phenomena in coupled van der Pol oscillators are good models to describe various higher-dimensional nonlinear phenomena in the field of natural science. However, in each one of them, van der Pol oscillators is either coupled by different method or has different feature. Therefore, investigation of synchronization phenomena observed in coupled oscillatory systems is an important issue.

The van der Pol oscillator is a simple circuit as shown in Fig. 1. It consists of an inductor, a capacitor and a nonlinear resistor.

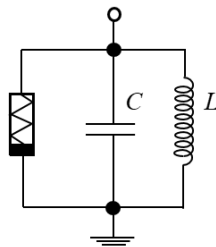


Figure 1: van der Pol oscillator.

In this study, we propose a new type of coupled van der Pol oscillators: Star structure connected to another oscillator. By carrying out computer simulations and theoretical analysis, the relationship of the model between synchronization phenomena and coupling strength is investigated.

2. Circuit Model

The proposed circuit is shown in Fig. 2. We use three van der Pol oscillators coupled as star structure that connected to another oscillator via resistors r . We investigate synchronization phenomena by changing coupling strength of the resistors.

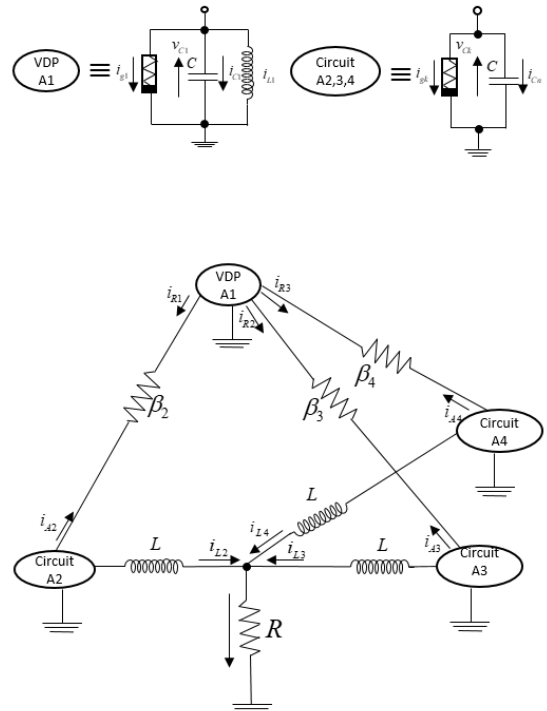


Figure 2: Circuit model.

With v_{C1}, v_{C2}, v_{C3} , and v_{C4} denote capacitor's voltage and i_{L1}, i_{L2}, i_{L3} , and i_{L4} denote inductor's electric current.

The circuit equations of VDP-A1 are given as follows:

$$\begin{aligned} C \frac{dv_{C1}}{dt} &= -i_{g1} - i_{L1} - i_{R1} - i_{R2} - i_{R3}, \\ L \frac{di_{L1}}{dt} &= v_1. \end{aligned} \quad (1)$$

The circuit equations of Circuit-A2, Circuit-A3, Circuit-A4 are given as follows:

$$\begin{aligned} C \frac{dv_{Ck}}{dt} &= -i_{gk} - i_{Lk} + i_{Rk}, \\ L \frac{di_{Lk}}{dt} &= v_k - R \sum_{m=2}^4 i_{Lm}. \end{aligned} \quad (2)$$

where:

$$i_{Rk} = \frac{v_1 - v_k}{r},$$

$$(k = 2, 3, 4).$$

The characteristics of the nonlinear resistors are defined as follows:

$$i_{gk} = -g_1 v_k + g_3 v_k^3. \quad (3)$$

By changing the variables and parameters:

$$\begin{aligned} t &= \sqrt{LC}\tau, v_k = \sqrt{\frac{g_1}{3g_3}} x_k, \\ i_{Lk} &= \sqrt{\frac{g_1 C}{3g_3 L}} y_k, \alpha = g_1 \sqrt{\frac{L}{C}}, \\ \beta &= \frac{1}{r} \sqrt{\frac{L}{C}}, \gamma = R \sqrt{\frac{C}{L}}, \end{aligned} \quad (4)$$

$$(k = 1, 2, 3, 4).$$

the normalized circuit equations of VDP-A1 are given as follows:

$$\begin{cases} \frac{dx_1}{d\tau} = \alpha \left(x_1 - \frac{1}{3} x_1^3 \right) - y_1 - \beta \left(3x_1 - \sum_{m=2}^4 x_m \right) \\ \frac{dy_1}{d\tau} = x_1. \end{cases} \quad (5)$$

the normalized circuit equations of Circuit-A2, Circuit-A3, Circuit-A4 are given as follows:

$$\begin{cases} \frac{dx_k}{d\tau} = \alpha \left(x_k - \frac{1}{3} x_k^3 \right) - y_k + \beta (x_1 - x_k) \\ \frac{dy_k}{d\tau} = x_k - \gamma \sum_{m=2}^4 y_m, \end{cases} \quad (6)$$

$$(k = 2, 3, 4).$$

where parameters α, β , and the γ denote nonlinearity, the resistors r , and the resistor R , respectively.

3. Simulation Results

For the computer simulations, we calculate Eqs. (2)-(3) by using Runge-Kutta method with the step size $h = 0.05$. When the parameters are fixed as $\alpha = 0.1, \gamma = 0.006$, we control synchronization phenomena of this circuit model by changing the coupling strengths $\beta_2, \beta_3, \beta_4$.

First, in the case of parameters $\beta_2, \beta_3, \beta_4$ are set to 0.015, Fig. 3 shows the attractor of each oscillator. Next, we slightly increase the parameters $\beta_2, \beta_3, \beta_4$ to the same value as 0.017, all four oscillators become in-phase as Fig. 4. When we only change β_2 to 0.005, the oscillator of Circuit A2 becomes anti-phase with other oscillators, when we change β_2, β_3 to 0.0005, oscillator of VDP-A1 becomes in-phase with oscillator of Circuit A2 and the oscillators of Circuit A2, A3, A4 become 3-phase synchronization. These results are shown in Figs. 5-6.

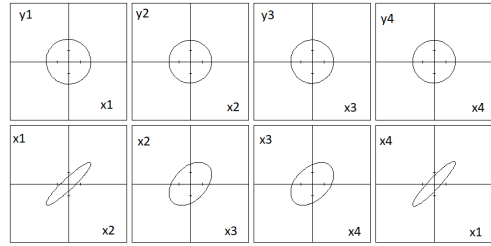


Figure 3: Phase differences ($\beta_2 = \beta_3 = \beta_4 = 0.015$).

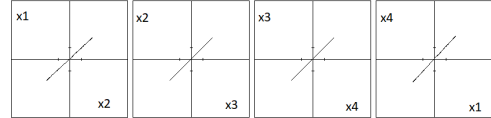


Figure 4: Phase differences ($\beta_2 = \beta_3 = \beta_4 = 0.017$).

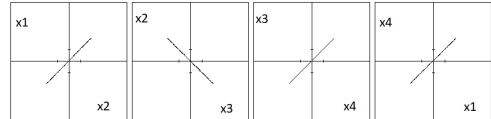


Figure 5: Phase differences ($\beta_2 = 0.005, \beta_3 = \beta_4 = 0.015$).

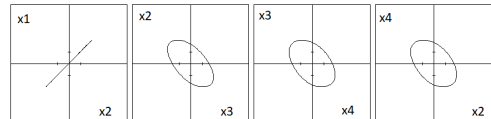


Figure 6: Phase differences ($\beta_2 = \beta_3 = 0.0005, \beta_4 = 0.015$).

Figures 7, 8 and 9 show the computer simulation results in each case when parameters $\beta_2, \beta_3, \beta_4$ are changed in ranges of values. From these result, we can control synchronization phenomena of this system by changing coupling strengths.

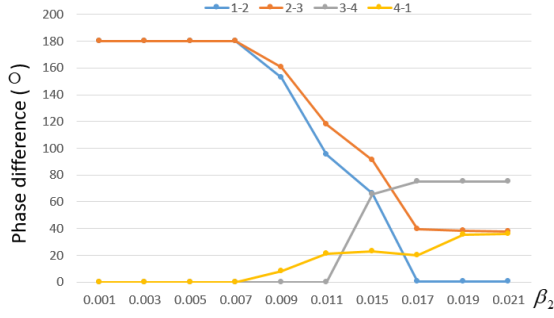


Figure 7: Phase differences in the case of changing β_2 .

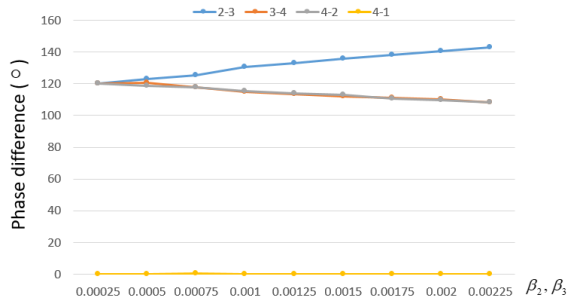


Figure 8: Phase differences in the case of changing β_2, β_3 .

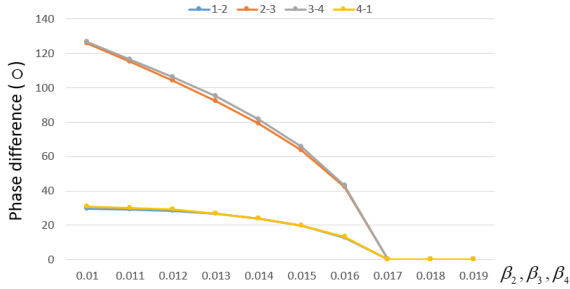


Figure 9: Phase differences in the case of changing $\beta_2, \beta_3, \beta_4$.

Therefore, we can control synchronization phenomena by changing the coupling strengths.

4. Theoretical Analysis

In this section, we apply theoretical analysis to confirm above computer simulation results by using averaging method for Eqs. (5) and (6). We assume that $x_{1,k}, y_{1,k}$ can be considered as below:

$$\begin{aligned} x_{1,k}(\tau) &= \rho_{1,k}(\tau) \cos(\tau + \theta_{1,k}(\tau)) \\ y_{1,k}(\tau) &= \rho_{1,k}(\tau) \sin(\tau + \theta_{1,k}(\tau)). \end{aligned} \quad (7)$$

Assign Eqs. (5)-(6) to Eq. (7), we obtain:

VDP-A1:

$$\begin{aligned} \dot{\rho}_1 &= \alpha(x_1 - \frac{1}{3}x_1^3) \cos \phi_1 - y_1 \cos \phi_1 \\ &\quad - \beta(3x_1 - \sum_{n=2}^4 x_n) \cos \phi_1 + x_1 \sin \phi_1 \equiv X_1 \\ \dot{\theta}_1 &= \frac{x_1 \cos \phi_1}{\rho_1} - \frac{\alpha(x_1 - \frac{1}{3}x_1^3) \sin \phi_1}{\rho_1} + \frac{y_1 \sin \phi_1}{\rho_1} \\ &\quad + \frac{\beta(3x_1 - \sum_{n=2}^4 x_n) \sin \phi_1}{\rho_1} - 1 \equiv Y_1. \end{aligned} \quad (8)$$

Circuit-A2, Circuit-A3, Circuit-A4:

$$\begin{aligned} \dot{\rho}_k &= \alpha(x_k - \frac{1}{3}x_k^3) \cos \phi_k - y_k \cos \phi_k \\ &\quad + \beta(x_1 - x_k) \cos \phi_k + x_k \cos \phi_k \\ &\quad - \gamma \sum_{n=2}^4 y_n \sin \phi_k \equiv X_k \\ \dot{\theta}_k &= \frac{x_k \cos \phi_k}{\rho_k} - \frac{\alpha(x_k - \frac{1}{3}x_k^3) \sin \phi_k}{\rho_k} + \frac{y_k \sin \phi_k}{\rho_k} \\ &\quad - \frac{\gamma \sum_{n=2}^4 y_n \cos \phi_k}{\rho_k} - 1 \equiv Y_k, \end{aligned} \quad (9)$$

where

$$\begin{aligned} \phi_k &= \tau + \theta_k \\ (k &= 2, 3, 4). \end{aligned}$$

By averaging Eqs. (8)-(9) over on period, as averaging method's theory, $\rho_{1,k}$ and $\theta_{1,k}$ can be considered as constant and the values of $\dot{\rho}_1, \dot{\theta}_1$ can be calculated as:

VDP-A1:

$$\begin{aligned} \dot{\rho}_1 &= \lim_{T \rightarrow \infty} \int_0^T X_1 d\tau \\ \dot{\theta}_1 &= \lim_{T \rightarrow \infty} \int_0^T Y_1 d\tau. \end{aligned} \quad (10)$$

Circuit-A2, Circuit-A3, Circuit-A4:

$$\begin{aligned} \dot{\rho}_k &= \lim_{T \rightarrow \infty} \int_0^T X_k d\tau \\ \dot{\theta}_k &= \lim_{T \rightarrow \infty} \int_0^T Y_k d\tau. \end{aligned} \quad (11)$$

By solving the above equations, Eqs. (10) and (11) are obtained:

VDP-A1:

$$\begin{aligned} \dot{\rho}_1 &= \frac{1}{2}\alpha\rho_1 - \frac{1}{8}\alpha\rho_1^3 + \beta\frac{3}{2}\rho_1 \\ &\quad + \sum_{n=2}^4 \frac{1}{2}\beta\rho_n \cos(\theta_n - \theta_1) \\ \dot{\theta}_1 &= \frac{1}{2} \sum_{n=2}^4 \frac{\rho_n}{\rho_1} \sin(\theta_n - \theta_1). \end{aligned} \quad (12)$$

Circuit-A2, Circuit-A3, Circuit-A4:

$$\begin{aligned} \dot{\rho}_k &= \frac{1}{2}\alpha\rho_k - \frac{1}{8}\alpha\rho_k^3 + \frac{1}{2}\beta\rho_1 \cos(\theta_1 - \theta_k) \\ &+ \frac{1}{2}\beta\rho_k - \sum_{n=2}^4 \frac{1}{2}\gamma\rho_n \cos(\theta_n - \theta_k) \\ \dot{\theta}_k &= \frac{1}{2} \sum_{n=2}^4 \frac{\rho_n}{\rho_k} \sin(\theta_k - \theta_n). \end{aligned} \quad (13)$$

In the steady state,

$\dot{\rho}_{1,k} = 0$ and $\dot{\theta}_{1,k} = 0$ must be satisfied. By solving Eqs. (12)-(13) we obtain:

$\frac{\rho_k}{\rho_1}$ as solution of below equation:

$$\frac{3}{2}\beta a^4 + \left(\frac{1}{2}\alpha - \frac{3}{2}\beta\right) a^3 - \left(\frac{1}{2}\alpha - \frac{1}{2}\beta - \frac{3}{2}\gamma\right) a - \frac{1}{2}\beta = 0. \quad (14)$$

For the phase difference:

$$\theta_2 - \theta_3 = \theta_3 - \theta_4 = \theta_4 - \theta_1 = 0.$$

These theoretical results correspond with the computer simulation results. Table 1 summarizes the comparison between theoretical and simulation results when the parameters α, γ are set as $\alpha = 0.05, \gamma = 0.006$ and parameter $\beta_{1,2,3}$ are changed together to 0.018, 0.02, 0.05. By solving Eq. (14), we can see that they match very well from below table.

Table 1: Comparison between theoretical and simulation results ($\alpha = 0.05, \gamma = 0.006$).

β	ρ_k/ρ_1	
	Theory	Simulation
0.018	0.885291	0.885314
0.02	0.890631	0.890658
0.05	0.936092	0.936131

5. Circuit Experiments

In this section, we build a real circuit to confirm these result above. We set $L = 20[\text{mH}], C = 33[\text{nF}]$ for each oscillator and change value of r . We also obtain the same synchronization from the circuit experiments. Figure 10 shows the result of oscillator 1, 2, 3 (Oscillator 2 is anti-phase). Figure 11 shows the result of oscillator 2, 3, 4. Figure 12 shows the result of oscillator 1, 2, 3.



Figure 10: Circuit experiment for $r_2 = 47[\text{k}\Omega], r_3 = r_4 = 2[\text{k}\Omega]$.

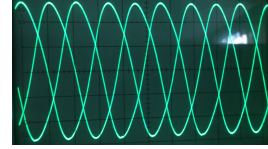


Figure 11: Circuit experiment for $r_2 = r_3 = 82[\text{k}\Omega], r_4 = 2[\text{k}\Omega]$.



Figure 12: Circuit experiment for $r_2 = r_3 = r_4 = 2[\text{k}\Omega]$.

6. Conclusions

In this study, we have investigated the synchronization phenomena in coupled oscillators containing star structure connected to another oscillator, and observe its synchronization phenomena by theoretical analysis, computer simulation and circuit experiment. In the next step, it is necessary to increase the number of oscillators and complete the theoretical analysis, and it is expected to bring us more interesting phenomena and we can find a good solutions for larger coupled systems.

References

- [1] K. Ueta, Y. Uwate and Y. Nishio, "Synchronization Phenomena in Complex Networks of van der Pol Oscillators", Proc. of NCSP'17, pp. 285-288, Mar. 2017.
- [2] Y. Uwate, Y. Nishio and R. Stoop, "Synchronization in Three Coupled van der Pol Oscillators with Different Coupling Strength", Proc. of NCSP'10, pp. 109-112, Mar. 2010.
- [3] F. Jhou, "Multistate and Multistage Synchronization of Hindmarsh-rose Neurons with Excitatory Chemical and Electrical Synapses", Proc. of IEEE, pp. 1335-1347, Jan. 2012.
- [4] W. Wessel, "Synchronization and Coupling Analysis: Applied Cardiovascular Physics in Sleep Medicine", Proc. of EMBC'13, pp. 6567-6570, Jul. 2013.